Feasibility Study of the Use of a Homemade Direct Powder Extrusion Printer to Manufacture Printed Tablets with an Immediate Release of a BCS II Molecule

O. Jennotte[1], N. Koch[1], A. Lechanteur[1], F. Rosoux[2], C. Emmerechts[2], E. Beeckman[2], Brigitte Evrard[1]

[1]Laboratory of Pharmaceutical Technology and Biopharmacy, Department of Pharmacy, Center for Interdisciplinary Research on Medicines (CIRM), University of Liege, 4000 Liege, Belgium.

[2]SIRRIS, Collective Centre of the Belgian Technology Industry, 4102, Liege Science Park, Belgium.

1. Introduction

3D printing is an additive manufacturing technique able to convert a computer-aided design model into a physical object by a layer by layer deposition of material [1]. This technique differs from traditional drug product manufacturing techniques in many ways. It allows to manufacture complex geometries [2], different dosage forms [3,4], drug products combining several incompatible active pharmaceutical ingredients (APIs) [5], complex drug delivery devices [6,7] and also original and unique shapes that increase patient compliance [8].

Among the various 3D printing techniques, fused-deposition modeling (FDM) is the most studied in pharmaceutical research due to its time-saving and cheap process, small size and accuracy [9]. FDM process consists of the extrusion of a filament made of thermoplastic polymers and one or several APIs and the deposition layer by layer of the molten material until the final printed shape is obtained. It allows to manufacture solid dosage forms with tailored doses [10], release [11] or shape [12] or different drugs [13], which proves its usefulness for personalized medicine [14,15]. However, this technique has some drawbacks. Prior to printing, the filament must generally be prepared by hot-melt extrusion (HME) that involves temperatures above T_g of polymers, which is not suitable for thermosensitive APIs. Moreover, filaments for FDM printing are challenging to obtain. Indeed, they must have specific mechanical properties, i.e., suitable brittleness and flexibility. In most cases, a certain amount of plasticizer has to be added to the formulation to adjust filament flexibility, which is not desired for the physical state stability of the drug. The filament diameter is another parameter to control. It must be homogeneous and can vary between 1.75 and 3.00 mm depending on the printer model used [16]. Filament diameter control often requires the use of expensive additional equipment, especially a conveyor belt, but also a melt pump or a filament maker [17]. Another method for filament loading is the immersion of a filament in a solution that contains the drug which penetrates into the filament by passive diffusion. This immersion method is suitable for thermosensitive drugs, but the drug loading is limited, generally to maximum 3% [18].

Direct powder extrusion 3D printing (DPE) may be useful to circumvent FDM drawbacks. This technique was first developed for the plastics industry [19]. It was recently implemented in the pharmaceutical field by Goyanes and his team who successfully manufactured itraconazole printed tablets with different grades of HPC [20]. The process implies the feeding of a powder

mixture into the printer hopper, heating and extrusion followed by the deposition, layer by layer of the molten material according to the previously digitally designed geometry. This one-step direct printing of powder avoids the need of filaments manufacture by HME which significantly reduces process time and waste. The thermal stress underwent by the API is also reduced since the DPE induces only one heating step, while there are two during FDM process, making DPE as a good alternative for the printing of thermosensitive drugs. Additionally, DPE can overcome the limitations encountered in HME regarding high drug loading. Indeed, the formulation of high drug loaded filaments usually requires additional excipients in order to obtain not too-brittle or too-flexible filament, which is not the necessary for DPE [21]. This technique has already proven its potential to print objects with various applications. For example, Goyanes *et al.* used different grades of hydroxypropylcellulose to manufacture printed tablets with a sustained release of itraconazole [20]. In another study, the ability of DPE to manufacture mini printed tablets with a high drug loading (25%) was demonstrated. The small size on the mini printed tablet allowed it to fit in a zero-size capsule in order to be combined with other mini printed tablets, oh other API, for treatment of disease requiring polypharmacy within a single dosage form [21]. Later, Malebari *et al.* investigated DPE for the printing of a combination of lopinavir/ritonavir in a pediatric dosage with HPMC and polyethylene glycol (PEG) in order to circumvent drug precipitation problem at intestinal pH observed with the administration of marketed drug Kaletra® [22]. Printed tablets were characterized by a zero-order sustained release drug during *in vitro* dissolution tests, which is promising for treating children with HIV. DPE also offers the possibility to print blends containing cyclodextrins as reported by Pistone *et al.* [23]. Indeed, authors successfully printed mixtures composed by niclosamide, hydroxypropyl-β-cyclodextrin (HPβCD) and PEG 6000. After *in vitro* dissolution tests, the solubility increase ability of HPβCD for poorly soluble drugs was highlighted.

Immediate release dosage forms, defined by the European Pharmacopoeia (edition 11.2, monograph 5.17.1) as forms allowing a drug dissolution of 80% within 45 minutes, were also printed using DPE, although the studied drugs belonged to BCS class I, having a high aqueous solubility [24–26]. To the best of our knowledge, no BCS II drugs with an immediate release has been successfully printed by DPE.

Therefore, the aim of this work was to print solid dosage forms allowing an immediate release of a BCS II drug, namely cannabidiol (CBD). This drug was chosen as a BCS II model drug for two reasons. Firstly, because this molecule has a low oral bioavailability, partly due to its low aqueous solubility (0.1 µg/mL in water) [27]. Secondly, CBD is being studied for many therapeutic properties, such as opioids use disorder, social anxiety, schizophrenia or cancers with a wide range of dosages varying from less than 1mg/kg/day to 50 mg/kg/day [28–30]. The majority of clinical studies for this promising drug are performed with liquid formulations, probably because it is the fastest and least expensive way to perform CBD dosage titrations. Indeed, conventional manufacturing methods such as tableting often hinder the rapid progress through pre-clinical studies, due to being dose inflexible, high costs and causing high waste [31,32]. DPE process could reduce time, cost and waste of these trials, given that it is sufficient

to feed the exact amount of powder mixture with a specific drug loading needed for the study. Moreover, formulations printed by DPE are solid forms, generally better accepted by the patients in comparison to liquid formulations [33,34].

A powder-based homemade printer was used to produce the printed tablets. CBD was previously mixed with Eudragit® E100 (E100) or Soluplus® (SOL), known for their ability to increase solubility of poorly soluble drugs, and Polyox® N10 (PEO) as a plasticizer, before being printed. The obtained printed tablets were evaluated in terms of immediate release and tested according to the European Pharmacopeia monograph for uncoated tablets, as to this day there is no official guidelines regarding the evaluation of the performances or the quality control of a final 3D printed product yet [35].

This study represents the first attempt to produce printed tablets containing a BCS II molecule with an immediate release, using a DPE process. It is expected to prove the interest and the robustness of this new 3D-printing technique for on-demand formulations. In the context of actual medicines shortages, DPE could provide a point-of-care rapid solution.

2. Material and methods

2.1. Materials

CBD was purchased from THC Pharm (Frankfurt, Germany). E100 (amino alkyl methacrylate copolymer, T_g: 50 °C, soluble in water at pH<5, gifted by Evonik, Germany) were used as matrix former. PEO (MW 100,000, gifted by Colorcon, UK), a semi-crystalline polymer (T_g = -67 °C and T_m = 65-70 °C) was used for its plasticizing effect. SOL (Polyvinyl caprolactam–polyvinyl acetate–polyethylene glycol graft copolymer, T_g = 67 °C) was kindly received from BASF Chemical Co. (Ludwigshafen, Germany).

2.2. Powder Flow Measurement

Powder mixtures must have an appropriate flow to be printed by DPE. Therefore, bulk and tapped density were measured according to the Ph. Eur. procedure 2.9.36 and the protocol was based on Lechanteur et al. work [36]. Briefly, a 10 mL cylinder was used and filled with the formulation. The bulk density was directly read in the cylinder. The tapped density was obtained with a tap density tester TD1 Sotax® (Aesch, Switzerland). The volume was read after 1250 taps. The values were determined as the mean of three replicates.

The Hausner's index and Carr's index were calculated with Eq. 1 and 2:

$$Hausner's\ Index = \frac{Bulk\ Density}{Tapped\ Density} \quad \text{Eq.1}$$

$$Carr's\ Index = \frac{Bulk\ Density - Tapped\ Density}{Bulk\ Density} \times 100 \quad \text{Eq.2}$$

Powder flowability can vary from very, very poor to excellent depending on the different index values *(Monograph 2.9.36-2, Eur. Ph. Edition 11.2)*.

2.3. Direct Powder Extrusion 3D Printing

In the present study, a homemade modified powder-based 3D printer was used (Fig. 1). The process is similar to conventional fused-deposition 3D printing but the printing is conducted directly from a powder mixture instead of a filament. It can be divided into three major steps. First, the powder mixture is loaded in a hopper which can hold up to 9 mL. The second step relies on the principle of a vertical hot-melt extruder. The mixture falls from the hopper and goes by gravity along a rotating Archimedes screw contained in a heated barrel until being extruded through a 0.4 mm nozzle. That implies that the powder must have an appropriate flow and a low viscosity at melting. However, kneading and heating powers of DPE are weaker than a classical extruder as DPE is composed by only one small-size screw without kneading elements, reducing DPE capacity to process highly viscous materials. Therefore, extrudability studies should be conducted in order to assess the printability of a powder blend. Indeed, powder with

poor flowability would not fall along the screw and molten materials that are too viscous would clog the nozzle.

For extrudable powder mixtures, the last step is the deposition of the molten material, layer-by-layer on a heated bed, until the final form is obtained.

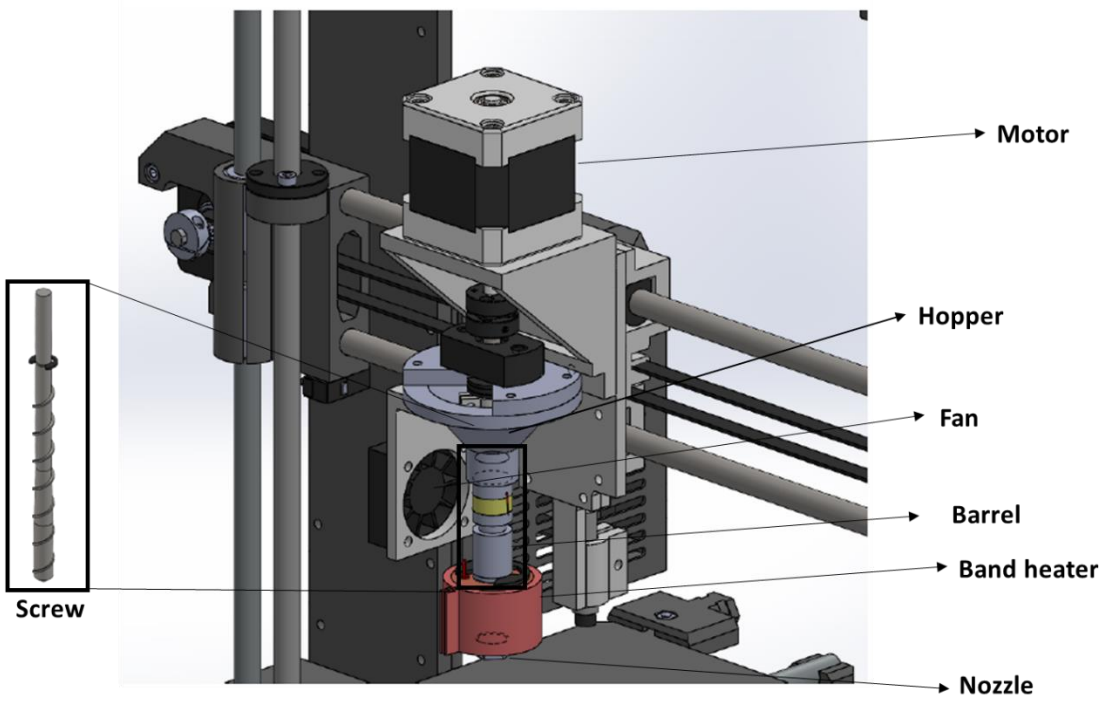

Figure 1 - Design of the printhead of the homemade modified powder-based 3D printer. The screw is enclosed in a barrel, heated by a band heater. A fan is directed between the barrel and a loading hopper to control the temperature profile along the extruder so that the powder mixture does not melt in an early way and can go by gravity along the screw until being melted and extruded by a 0.4 mm nozzle.

E100 or SOL were used as polymeric carriers for the manufacturing of ASDs. As these two polymers are not printable on their own because of their brittleness, PEO was added to each formulation as a plasticizer.

As explained above, DPE printer must be able to extrude the powder mixture through the nozzle in order to deposit it layer-by-layer to obtain the desired printed object. Therefore, extrudability studies were performed on different E100/PEO and SOL/PEO ratios, each combined with 10% of CBD (Table 1).

Prior to mixing, every component was sieved through a 0.4 mm mesh sieve to provide a better size uniformity between the different powders. The powder mixtures were performed using a mortar and a pestle until no aggregated particles were observed. Extrudability tests were performed as follows: each powder mixture was introduced in the printer loading hopper (Fig. 1) and the screw was rotated for 180 seconds at 16 rpm and a temperature of 155 °C. After this time, obtained filaments were measured. The longer the filament, the more extrudable the powder mixture.

Table 1 - Composition of powder mixtures

Formulations	CBD (%)	PEO (%)	E100 (%)	SOL (%)
F1	10	72	18	0
F2	10	67.5	22.5	0
F3	10	63	27	0
F4	10	58.5	31.5	0
F5	10	54	36	0
F6	10	49.5	40.5	0
F7	10	72	0	18
F8	10	67.5	0	22.5
F9	10	63	0	27
F10	10	58.5	0	31.5
F11	10	54	0	36
F12	10	49.5	0	40.5

The different powder mixtures gathered in Table 1 were printed with the following parameters: printing speed 20 mm/s, layer height 0.1 mm, heated bed T° 25 °C and printing T° 155 °C. The printhead was disassembled and cleaned after the printing of each formulation in order to prevent the cross-mixing between them. Once printed, the dimensions of the cylinders were taken using a digital caliper to evaluate the printer precision.

The printed tablets were designed as cylindrical objects (diameter = 15 mm, height = 6.2 mm) using Tinkercad™ free online software (Autodesk, CA, USA). Cylinder dimensions and infill (20%) were set to obtain printed forms of 650 mg per printed tablet which corresponds to an equivalent of 65 mg of CBD. This dosage was chosen in order to be within the dose range tested in the different studies found in the literature [31]. The obtained .stl files were converted to gcode files using the software Ultimaker Cura, version 4.11.0 (Ultimaker, The Netherlands).

2.4. Drug Content of Printed Tablets

Since the formulations are exposed to high temperatures during their production, the drug content was measured after printing. Samples of 20-30 mg were cut from the printed tablets and dissolved in acetonitrile prior to HPLC analysis. A validated reverse phase high-performance liquid chromatography (HPLC) analytical method, described in a previous work, was used (Koch et al., 2020). The HPLC equipment consisted of an Agilent® 1100 (Santa Clara, USA) with OpenLab CDS lC ChemStation version C.01.05 as the software. The mobile phase was composed of water/acetonitrile (38/62% (v/v)) and the column was Zorbax® C18 300 SB with particles of 3.5 µm (150 mm x 4.6 mm ID). The flow rate was set at 1.0 mL/min and the temperature was kept at 30 °C. The

injection volume was 20.0 µL, the chromatographic run time was 10 min and the detection of CBD was made at a wavelength of 240 nm. The measurements were carried out in triplicate.

2.5. Characterization of Printed Tablets

As there is still no monograph concerning the printed forms in the European Pharmacopeia, the printed cylinders were characterized with tests according to the monograph dedicated to the uncoated tablets of the European Pharmacopeia Edition 11.2.

2.4.1 Friability Test (Monograph 2.9.7 Eur. Ph. Edition 11.2)

Ten printed tablets of each formulation were dusted, weighed and placed in the drum of a Friabilator USP F2 Sotax® (Aesch, Switzerland). After 100 rotations of the drum, the printed tablets were dusted, weighed again and the target mass loss was less than 1% (Monograph 2.9.7. Eur. Ph. Edition 11.2).

2.4.2 Tensile Strength

The tensile strength of printed tablets of each formulation was determined in triplicate using the breaking force (F) measured by a crushing strength tester Pharmatron MT-50 Sotax® (Aesch, Switzerland) and with the following equation:

$$TS = \frac{2F}{\Pi D t}$$

Where:

D is the diameter

t is the overall thickness

2.4.3 Mass Variation (Monograph 2.9.40 Eur. Ph. Edition 11.2)

Ten printed tablets of each formulation were individually weighted and the Acceptance Value (AV) was calculated using the following equation (Monograph 2.9.40. Eur. Ph. Edition 11.2):

$$AV = | M - X | + 2.4s$$

Where:

M is a reference value which depends on X

X is the mean of the individual content, expressed as a percentage of the theoretical value of CBD

s is the sample standard deviation

The target AV was lower than 15.00.

2.4.4 Uniformity of Mass (Monograph 2.9.5 Eur. Ph. Edition 11.2)

Ten printed tablets of each formulation were weighed and the average mass was determined. The test was considered as conform if not more than two of the individual masses deviate from the average mass by more than 5% of deviation and none deviate by more than twice that percentage.

2.4.5. X-ray Diffraction

In order to evaluate the physical state of CBD once printed, disks (23.12 mm diameter x 1.00 mm height) made of the printable powder mixtures of were printed and analyzed. X-ray diffractograms were collected using a Bruker D8 TWIN-TWIN diffractometer in Bragg-Brentano configuration (Cu Kalpha radiation, variable divergence slit V6, sample rotation 15 rpm) with a Lynxeye XET detector in 1D mode (192 channels) and a total scan time of 15 or 30 min for a 0.02° step size.

2.6. Dissolution Tests

The *in vitro* dissolution experiments were conducted using USPII paddle method apparatus AT7 (Sotax®, Switzerland). One printed tablet of each formulation was placed in a sinker containing 500 mL of HCl 0.1 N at a pH value of 1.6 for two hours followed by two hours with an addition of Na_3PO_4 0.2 M. The pH value was adjusted to 6.8 with addition of HCl 1 N or NaOH 2 N within a time interval of less than 5 minutes. The stirring speed was 100 rpm and the temperature was maintained at 37 °C. The samples were analyzed by HPLC-UV and replaced by fresh medium (2.9.3. Ph. Eur. Ed. 11.2). Every formulation was analyzed in triplicate.

2.7. Dynamic Light Scattering

Solutions composed of the polymers and/or CBD in acidic and neutral media were characterized by Dynamic Light Scattering (DLS) using a Malvern Zetasizer® (Nano ZS, Malvern Instrument, UK) at 25 °C with a fixed angle of 90° (n=3) in order to measure their particle size during dissolution.

3. Results and discussion

3.1. Powder Flow Measurement

The flowability of each powder formulation has been measured since it influences the powder progression along the screw. As shown in Table 2, flowability of the powders varies from fair to excellent by decreasing the percentage of PEO. These measurements show that the used powder in this study possesses appreciable flowability, which is necessary to assure appropriate material extrusion.

Table 2 - Carr's and Hausner's indexes and resulting flowability for each formulation

Formulations	Carr's Index	Hausner' s Index	Flowability
F1	10.00	1.11	Excellent
F2	11.11	1.13	Good
F3	12.22	1.14	Good
F4	13.33	1.15	Good
F5	16.67	1.20	Fair
F6	17.78	1.22	Fair
F7	8.89	1.10	Excellent
F8	10.00	1.11	Excellent
F9	12.22	1.14	Good
F10	14.44	1.17	Good
F11	17.78	1.22	Fair
F12	17.78	1.22	Fair

3.2. 3D Printing of Powder Mixtures

Prior to the printing step, powder mixtures containing increasing proportions of E100/PEO or SOL/PEO each combined with 10% of CBD were tested to determine if they were extrudable within the modified printer head. Every formulation was extrudable, except for F5 and F6 which clogged the nozzle, probably because of a too high viscosity. Filament lengths obtained after extrusion of the other formulations are gathered in Table 3. Mixtures containing SOL could be extruded with a maximum of 40.5% SOL while mixtures containing E100 could be extruded with a maximum of 31.5% E100. The filament length decreased with the increase of the E100 or SOL proportion. This highlighted the strong influence of the composition of the formulation on the extrudability. Indeed, small reductions in the proportions of PEO led to large reductions in the amount of extruded material. As the flowing was good for every formulation, the difference of extrudability would be due to E100 and SOL viscosity at the printing temperature. Indeed, these two polymers have already been reported as having a relatively high viscosity when melted, with a higher viscosity of E100 compared to SOL [37].

Table 3 - Length of filament obtained for each formulation after extrudability studies

Formulation	F1	F2	F3	F4	F5	F6	F7	F8	F9	F10	F11	F12
Filament length (cm)	36	30	22	7	0	0	47	39	31	10	5	3

The modified powder-based printer was used to print the extrudable powder mixtures (F1 to F4 and F7 to F12). All mixtures could be printed, except for F4, F10, F11 and F12 which resulted in an incomplete shape compared to the digital model. This is explained by the poor extrudability of these mixtures, as observed by the little amounts of material extruded during the extrudability study. For these formulations, the printing speed should be decreased in order to match the nozzle throughput, but the printing time per tablet would be too long so these formulations were withdrawn.

The time from loading the powder until obtaining the final cylinder was about 6 minutes which is in the time range of different printed tablets produced by FDM [38]. Moreover, the losses are negligible compared to those generated by more conventional 3D printing techniques such as FDM. Indeed, it implies an additional HME step for the filament production that generates material loss. This makes DPE a promising technique for the production of small batches intended for clinical studies or personalized medicine, for example.

3.3. Characterization of Printed Tablets

The diameter and height of ten printed tablets of each formulation were measured and the deviation from the dimensions of the digital model is shown in Table 4. All the printed tablets had a deviation of the diameter from -5.00 ± 2.17% to 1.47 ± 0.14% compared to the digital model. Regarding the height, the printed tablets had a deviation ranging from -3.44 ± 1.23% to -0.34 ± 0.17. These low deviations dimensions of the printed cylinders compared to the digital model highlight the precision of this homemade direct powder extruder.

The monograph concerning uncoated tablets of the European Pharmacopeia was used to characterize the printed tablets as there is no existing monograph for the printed formulations. Since powder mixtures are exposed to high temperatures during the printing process, the drug recovery measurement is important, as these temperatures can degrade the API. Results of CBD recovery are shown on Table 4 and suggest that there is no drug degradation in formulations, as CBD recovery is ranging from 95.77 ± 0.66% to 99.20 ± 2.33. Drug recoveries are in accordance with TGA analysis (appendix) as printing temperatures did not exceed the degradation temperature of CBD (220 °C), E100 (289 °C), PEO (389 °C) and SOL (290 °C). These results indicated that the processing conditions did not significantly impact the CBD chemical stability in the printed tablets.

The *friability* and the *tensile strength* are two important parameters concerning the study of the integrity of oral solid dosage forms during the production, transport and handling by the patient. Moreover, these two parameters especially the tensile strength have an influence of the dissolution of the dosage forms. Indeed, a printed tablet with a high tensile strength will dissolve

slower than one with a low tensile strength as the structure is harder to disintegrate. The results on Table 4 show that the mass loss during the friability test was <1% for each formulation and met the Eur. Ph. specifications. Compared to the standard techniques for the manufacturing of oral solid dosage forms such as tableting, or other 3D printing techniques like drop-on-powder 3D printing, DPE allows the production of products with a poor friability without additional steps or excipients [39]. There is no requirement concerning the tensile strength and the values were comparable to another study focused on DPE [20].

Table 4 - Characterization of printed tablets

Formulations	Cannabidiol Recovery (%)	Diameter[a] (%) (n=10)	Height[a] (%) (n=10)	Friability* (%)	Tensile Strength
F1	96.75 ± 1.05	97.00±1.15	98.57±1.71	0.25	0.97 ± 0.23
F2	98.12 ± 3.02	96.51±0.75	98.54±0.39	0.17	1.01 ± 0.17
F3	95.77 ± 0.66	95.00±2.17	99.66±0.17	0.22	0.99 ± 0.11
F7	97.15 ± 1.33	101.47±0.14	97.66±1.16	0.02	0.85 ± 0.37
F8	99.20 ± 2.33	101.00±0.51	98.02±0.74	0.09	0.91 ± 0.03
F9	96.00 ± 1.58	98.79±0.87	96.56±1.23	0.12	0.87 ± 0.21

a% = printed model/digital model (measured in triplicate). * = measured on ten printed tablets.

Both *mass variation* and *uniformity of mass* tests were performed to ensure that the mass of all the produced printed tablets was within limits defined by the European Pharmacopeia. Figure 7 represents the mean mass measured on ten printed tablets of each formulation and the acceptance value for each formulation. As it can be observed, printed tablets mean masses differ between each formulation, going from 616.28 mg to 660.99 mg. Such deviations have already been reported in the literature [20,23,40].

However, every formulation was in accordance with the mass variation test as every acceptance value was below 15.00. Concerning the uniformity of mass test, the average mass of ten printed tablets of each formulation was calculated. In order to be in compliance European Pharmacopeia requirements of the uniformity of mass test, no printed tablet must have a deviation from the average mass superior to 10% and not more than two printed tablets of each formulation must deviate from more than 5%. The results of our study showed deviations of respectively -9.21% and +6.84% for the most under and over-weighted tablets. Moreover, no more than two printed tablets per formulation deviated from more than 5% of the average mass. The test was therefore compliant and proved the ability of the DPE to produce printed tablets with adequate reproducibility.

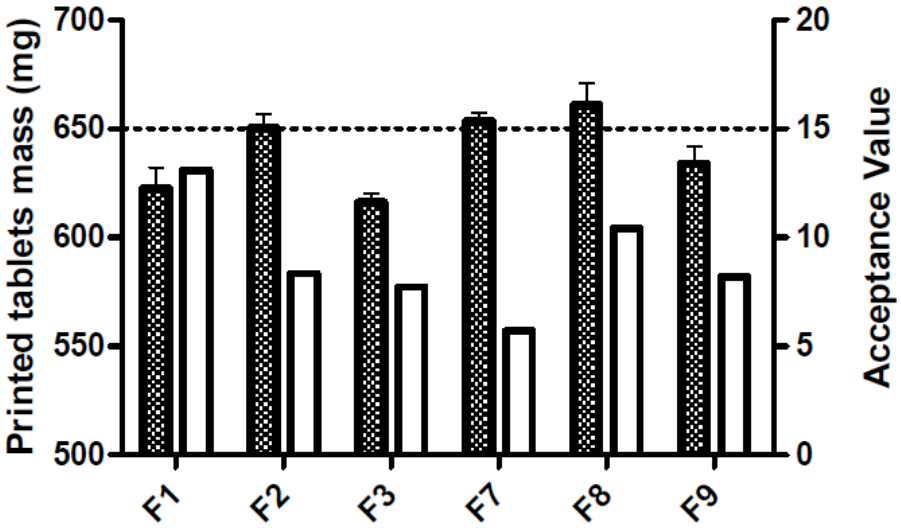

Figure 2 - Mass of the printed tablet of the six formulations (mean and SD, n = 10) represented by the dashed columns and the acceptance value for each formulation represented by the empty columns (measured on ten printed tablets). The target mass is represented by the dashed line.

X-ray diffraction was used to study the physical state of CBD, polymers and printed tablets. CBD and PEO showed sharp peaks confirming their crystalline or semi-crystalline nature, respectively (Fig. 3). The pattern of E100 showed a wide halo, characteristic of amorphous compounds. The characteristic peaks around ten of CBD were not found on formulation patterns, indicating a total amorphization of the drug during the printing process. DPE does not always induce a drug total amorphization as formulations remain only a few minutes at high temperature while conventional methods to transform a drug in its amorphous state generally involve a dissolution of the drug in specifics solvent or prolonged contact of the drug at high temperatures [20,22,24,41,42]. This implies that our homemade printed is suitable for the production of amorphous formulations of CBD.

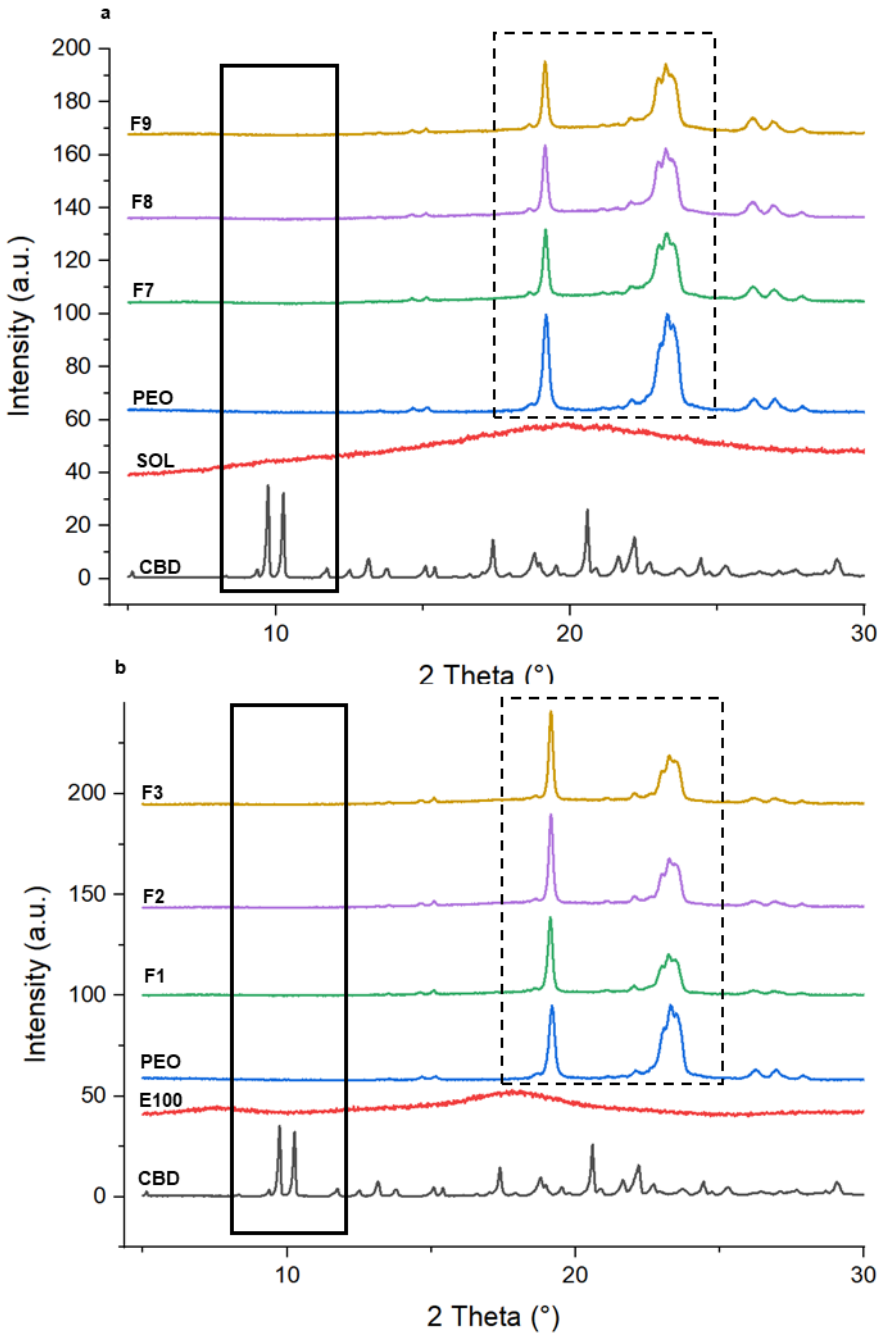

Figure 3 - XRD patterns of crystalline CBD, E100, SOL, PEO and the printed disks composed of F1, F2, F3, F7, F8 and F9. The diffractograms of E100 and SOL show a halo confirming the amorphous state of these polymers. The dotted frame shows the absence of the characteristic peaks of crystalline CBD at about 10° in each formulation, which means that CBD is completely amorphous in all printed disks. The continuous line frame highlights the semi-crystalline character of PEO which shows characteristic peaks at about 19° and 24°. These peaks are also present in the printed disks, suggesting rapid recrystallization of PEO.

3.4. In Vitro Dissolution Tests

Dissolution tests were performed in acidic conditions at pH value of 1.6 during two hours followed by two hours at pH value of 6.8. This was done to evaluate the ability of tested formulations to dissolve CBD and maintain a supersaturated solution in both acidic and neutral pH. These dissolutions tests were conducted based on a study that highlighted the tendency of CBD to be better absorbed in the upper intestine (at pH 6.8) leading to the need to dissolve a maximum of CBD in stomach conditions (at pH 1.6) [43].

Formulations containing SOL and PEO (F7, F8 and F9) did not allow an increase of CBD solubility during the four hours of dissolution test (data not shown). Indeed, a gel was formed at the layer surface of the printed tablets once in contact with the dissolution medium (Fig. 4). This gel behavior has already been described in the literature for both SOL and PEO [44,45]. These polymers have a strong affinity for water. Once in contact, the strength of the water-polymer bonds surpasses that of the polymer-polymer bonds, allowing water to penetrate between the polymer chains, causing swelling and the formation of a gel layer. This layer slows the erosion of both polymer and drug. Addition of salts or disintegrants have already been studied in ASDs with SOL to break the gel network and increase the drug dissolution rate [46].

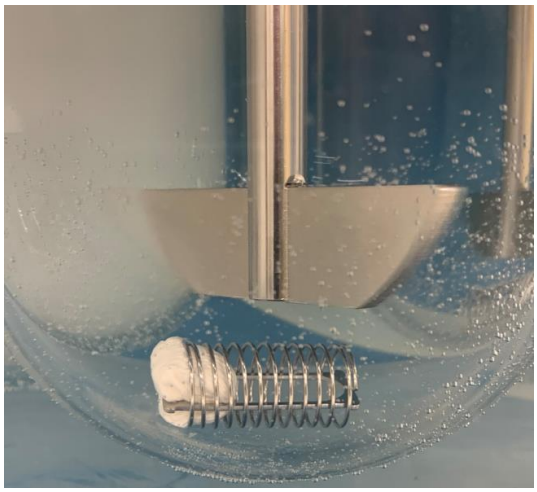

Figure 4 - Gel mass formed by F7 once in contact with the acidic dissolution medium.

On the other hand, formulations containing E100 and PEO (F1, F2 and F3) allowed an immediate release of CBD. Indeed, 95.27% ± 0.86, 87.40% ± 2.01 and 92.47% ± 5.76 of CBD was released after 45 minutes from F1, F2 and F3, respectively. This high dissolution rate suggested that E100 broke the gel layer formed by PEO. Indeed, this polymer possesses amino functions which are ionized at pH less than 5, allowing a fast dissolution. Moreover, the supersaturated solution was maintained at both pH. This concentration upkeep was not expected as the amino functions of E100 are not ionized when pH is above 5, making this polymer not soluble.

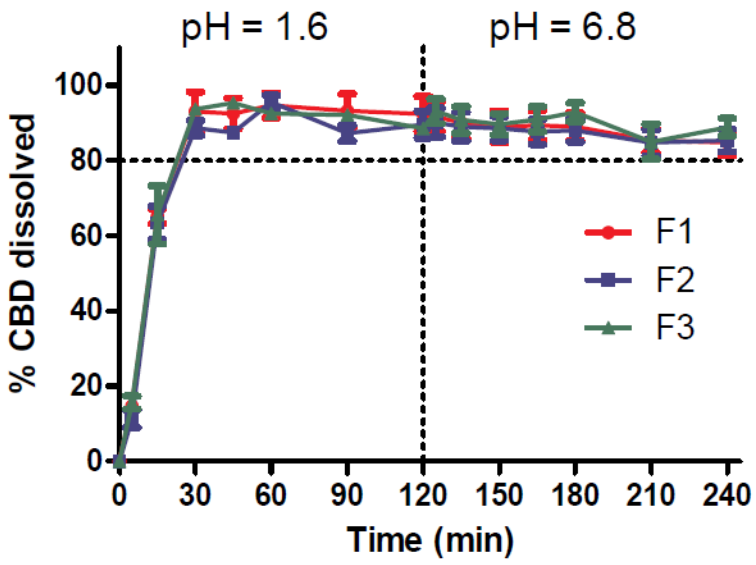

Figure 5 - Dissolution profile of formulations containing E100 in an acidic medium (left of the dotted vertical line) and in a neutral medium (right of the dotted vertical line).

This upkeep of CBD concentration in both media could be explained by the mechanism of dissolution of E100. Authors have demonstrated that Eudragit® EPO, which has the same composition as E100, makes it possible to dissolve poorly water-soluble molecules, in addition to maintaining the amorphous state of these molecules, by forming micelles in an acidic medium [47]. We have verified this hypothesis by DLS analysis as shown in Figure 6. The dissolution of E100 alone in the acidic dissolution medium composed of HCl 0.1 N at a pH value of 1.6, a major population is measured at about 10 nm which is in the range of classic micelles which is 5-100 nm (Fig. 6.a) [48]. After pH adjustment at a value of 6.8, no major population could be observed suggesting micelles disorganization (Fig. 6.b). However, the dissolution of E100 and PEO in neutral medium at a pH value of 6.8 seemed to stabilize the micelles formed by E100 (Fig. 6.c). This was also observed with the dissolution of one of the printed tablets composed with these two polymers (F3, Fig. 6.d and 6.e). Single particles population at about 500 nm was observed in both acidic and neutral media. The particles size difference between the solutions composed of E100 and PEO and the solutions composed of F3 is explained by the solubilization of into the core of E100/PEO particles [47].

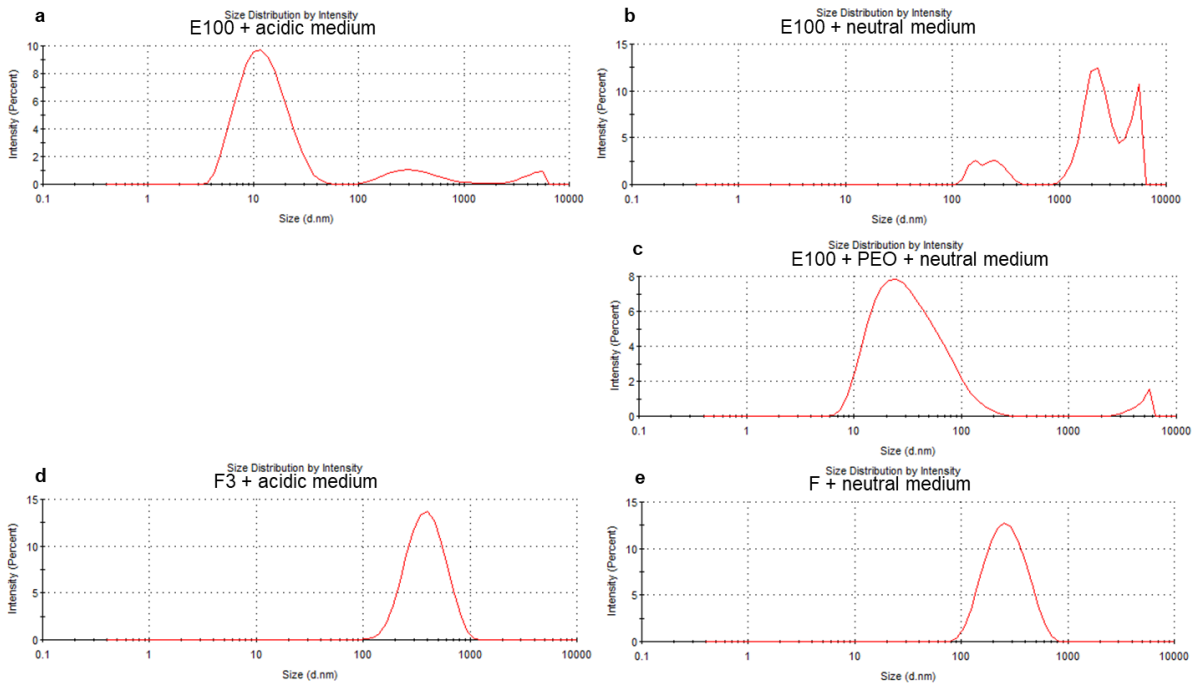

Figure 6 – Particle size distribution of a. E100 dissolved in acidic medium at pH 1.6, b. E100 dissolved in neutral medium at pH 6.8, c. E100 and PEO dissolved in neutral medium at pH 6.8, d. F3 composed of CBD/PEO/E100 (10/63/27) dissolved in acidic medium at pH 1.6 and e. F3 dissolved in neutral medium at pH 6.8.

4. Conclusion

For the first time, printed tablets containing an amorphous solid dispersion allowing an immediate release (80% in 45 minutes) of a BCS II molecule were manufactured by DPE. The printing was done directly from powder mixtures without the need of developing a printable filament, reducing time, cost and difficulty of the printing process.

The printed tablets were composed either of E100/PEO or SOL/PEO, at different ratios, in combination with 10% of CBD. Only the formulations containing E100 allowed an increase of aqueous solubility and dissolution rate of CBD, confirming the importance of polymers screening.

In addition to the improved performance of the aqueous solubility of CBD, printed tablets complied with the tests of the monograph concerning uncoated tablets of the European Pharmacopeia.

The results obtained in this study highlighted the ability of DPE for the production and shaping of amorphous solid dispersions with an immediate release and a suitable quality. This may be promising for the on-demand manufacture of small batches by community pharmacies, hospitals or to conduct clinical trials since the time and waste of the process is greatly reduced compared to conventional manufacturing techniques.

5. Acknowledgments

The authors wish to acknowledge FEDER funds for the support in SOLPHARE FEDER project (884148-329407) and the Fonds Léon Fredericq for the support in project 2021-2022-12. The authors also wish to thank Wenda Lazzari and Astrid Couturier (Mithra CDMO) for the loan and the support of the melt pump.

6. References

1. Omari S, Ashour EA, Elkanayati R, Alyahya M, Almutairi M, Repka MA. Formulation development of loratadine immediate- release tablets using hot-melt extrusion and 3D printing technology. J Drug Deliv Sci Technol [Internet]. Elsevier B.V.; 2022;74:103505. Available from: https://doi.org/10.1016/j.jddst.2022.103505

2. Lamichhane S, Park JB, Sohn DH, Lee S. Customized novel design of 3D printed pregabalin tablets for intra-gastric floating and controlled release using fused deposition modeling. Pharmaceutics. 2019;11.

3. Jiang H, Fu J, Li M, Wang S, Zhuang B, Sun H, et al. 3D-Printed Wearable Personalized Orthodontic Retainers for Sustained Release of Clonidine Hydrochloride. AAPS PharmSciTech. AAPS PharmSciTech; 2019;20:1–10.

4. Trenfield SJ, Awad A, Madla CM, Hatton GB, Firth J, Goyanes A, et al. Shaping the future: recent advances of 3D printing in drug delivery and healthcare. Expert Opin Drug Deliv [Internet]. Taylor & Francis; 2019;16:1081–94. Available from: https://doi.org/10.1080/17425247.2019.1660318

5. Gioumouxouzis CI, Baklavaridis A, Katsamenis OL, Markopoulou CK, Bouropoulos N, Tzetzis D, et al. A 3D printed bilayer oral solid dosage form combining metformin for prolonged and glimepiride for immediate drug delivery. Eur J Pharm Sci [Internet]. Elsevier; 2018;120:40–52. Available from: https://doi.org/10.1016/j.ejps.2018.04.020

6. Dumpa N, Butreddy A, Wang H, Komanduri N, Bandari S, Repka MA. 3D printing in personalized drug delivery: An overview of hot-melt extrusion-based fused deposition modeling. Int J Pharm [Internet]. Elsevier B.V.; 2021;600:120501. Available from: https://doi.org/10.1016/j.ijpharm.2021.120501

7. Beg S, Almalki WH, Malik A, Farhan M, Aatif M, Rahman Z, et al. 3D printing for drug delivery and biomedical applications. Drug Discov Today [Internet]. Elsevier Ltd; 2020;25:1668–81. Available from: https://doi.org/10.1016/j.drudis.2020.07.007

8. Vaz VM, Kumar L. 3D Printing as a Promising Tool in Personalized Medicine. AAPS PharmSciTech. AAPS PharmSciTech; 2021;22.

9. Rahim TNAT, Abdullah AM, Md Akil H. Recent Developments in Fused Deposition Modeling-Based 3D Printing of Polymers and Their Composites. Polym Rev [Internet]. Taylor & Francis; 2019;59:589–624. Available from: https://doi.org/10.1080/15583724.2019.1597883

10. Crișan AG, Iurian S, Porfire A, Rus LM, Bogdan C, Casian T, et al. QbD guided development of immediate release FDM-3D printed tablets with customizable API doses. Int J Pharm. 2022;613.

11. Shi K, Slavage JP, Maniruzzaman M, Nokhodchi A. Role of release modifiers to modulate drug release from fused deposition modelling (FDM) 3D printed tablets. Int J Pharm [Internet]. Elsevier B.V.; 2021;597:120315. Available from: https://doi.org/10.1016/j.ijpharm.2021.120315

12. Goyanes A, Robles P, Buanz A, Basit AW, Gaisford S. Effect of geometry on drug release from 3D printed tablets. Int J Pharm [Internet]. Elsevier B.V.; 2015;494:657–63. Available from: http://dx.doi.org/10.1016/j.ijpharm.2015.04.069

13. Pereira BC, Isreb A, Forbes RT, Dores F, Habashy R. ' Temporary Plasticiser ': A novel solution to fabricate 3D printed patient- centred cardiovascular ' Polypill ' architectures. Eur J Pharm Biopharm [Internet]. Elsevier; 2019;135:94–103. Available from: https://doi.org/10.1016/j.ejpb.2018.12.009

14. Khalid GM, Billa N. Solid Dispersion Formulations by FDM 3D Printing—A Review. Pharmaceutics. 2022;14.

15. Sandler N, Preis M. Printed Drug-Delivery Systems for Improved Patient Treatment. Trends Pharmacol Sci [Internet]. Elsevier Ltd; 2016;37:1070–80. Available from: http://dx.doi.org/10.1016/j.tips.2016.10.002

16. Jennotte O, Koch N, Lechanteur A, Evrard B. Three-dimensional printing technology as a promising tool in bioavailability enhancement of poorly water-soluble molecules: A review. Int J Pharm [Internet]. Elsevier B.V.; 2020;580:119200. Available from: https://doi.org/10.1016/j.ijpharm.2020.119200

17. Parulski C, Jennotte O, Lechanteur A, Evrard B. Challenges of fused deposition modeling 3D printing in pharmaceutical applications: Where are we now? Adv Drug Deliv Rev. 2021;175.

18. Fernández-García R, Prada M, Bolás-Fernández F, Ballesteros MP, Serrano DR. Oral Fixed-Dose Combination Pharmaceutical Products: Industrial Manufacturing Versus Personalized 3D Printing. Pharm. Res. Springer; 2020.

19. Liu X, Chi B, Jiao Z, Tan J, Liu F, Yang W. A large-scale double-stage-screw 3D printer for fused deposition of plastic pellets. J Appl Polym Sci. 2017;134:1–9.

20. Goyanes A, Allahham N, Trenfield SJ, Stoyanov E, Gaisford S, Basit AW. Direct powder extrusion 3D printing: Fabrication of drug products using a novel single-step process. Int J Pharm. 2019;567.

21. Sánchez-Guirales SA, Jurado N, Kara A, Lalatsa A, Serrano DR. Understanding direct powder extrusion for fabrication of 3d printed personalised medicines: A case study for nifedipine minitablets. Pharmaceutics. 2021;13.

22. Malebari AM, Kara A, Khayyat AN, Mohammad KA, Serrano DR. Development of Advanced 3D-Printed Solid Dosage Pediatric Formulations for HIV Treatment. Pharmaceuticals. 2022;15:1–15.

23. Pistone M, Racaniello GF, Arduino I, Laquintana V, Lopalco A, Cutrignelli A, et al. Direct cyclodextrin-based powder extrusion 3D printing for one-step production of the BCS class II model drug niclosamide. Drug Deliv Transl Res [Internet]. Springer US; 2022;12:1895–910. Available from: https://doi.org/10.1007/s13346-022-01124-7

24. Fanous M, Gold S, Muller S, Hirsch S, Ogorka J, Imanidis G. Simplification of fused deposition modeling 3D-printing paradigm: Feasibility of 1-step direct powder printing for immediate release dosage form production. Int J Pharm [Internet]. Elsevier; 2020;578:119124. Available from: https://doi.org/10.1016/j.ijpharm.2020.119124

25. Mendibil X, Tena G, Duque A, Uranga N, Campanero MÁ, Alonso J. Direct powder extrusion of paracetamol loaded mixtures for 3d printed pharmaceutics for personalized medicine via low temperature thermal processing. Pharmaceutics. 2021;13.

26. FDA. Dissolution Testing and Acceptance Criteria for Immediate-Release Solid Oral Dosage Form Drug Products Containing High Solubility Drug Substances Guidance for Industry. 2018;8. Available from: http://www.fda.gov/Drugs/GuidanceComplianceRegulatoryInformation/Guidances/default.htm%0Afile:///C:/Users/ASUS/Desktop/Rujukan PhD/Drug Release/1074043 FNL_clean.pdf

27. Koch N, Jennotte O, Gasparrini Y, Vandenbroucke F, Lechanteur A, Evrard B. Cannabidiol aqueous solubility enhancement: Comparison of three amorphous formulations strategies using different type of polymers. Int J Pharm [Internet]. Elsevier; 2020;589:119812. Available from: https://doi.org/10.1016/j.ijpharm.2020.119812

28. Bergamaschi MM, Helena Costa Queiroz R, Hortes M, Chagas N, Chaves Gomes De Oliveira D, De Martinis BS, et al. Cannabidiol Reduces the Anxiety Induced by Simulated Public Speaking in Treatment-Naı¨veNaı¨ve Social Phobia Patients. Neuropsychopharmacology [Internet]. 2011;36:1219–26. Available from: www.neuropsychopharmacology.org

29. Heider CG, Itenberg SA, Rao J, Ma H, Wu X. Mechanisms of Cannabidiol (CBD) in Cancer Treatment: A Review. 2022; Available from: https://doi.org/10.3390/biology11060817

30. McGuire P, Robson P, Cubala WJ, Vasile D, Morrison PD, Barron R, et al. Cannabidiol (CBD) as an adjunctive therapy in schizophrenia: A multicenter randomized controlled trial. Am J Psychiatry. 2018;175:225–31.

31. Millar S, Stone N, Bellman Z, Yates A, England T, Sophie Millar CA. A systematic review of cannabidiol dosing in clinical populations. Artelo Biosci Biotechnol Biol Sci Res Counc. 2019;

32. Seoane-Viaño I, Trenfield SJ, Basit AW, Goyanes A. Translating 3D printed pharmaceuticals: From hype to real-world clinical applications. Adv Drug Deliv Rev [Internet]. The Authors; 2021;174:553–75. Available from: https://doi.org/10.1016/j.addr.2021.05.003

33. Vasconcelos T, Sarmento B, Costa P. Solid dispersions as strategy to improve oral bioavailability of poor water soluble drugs. Drug Discov Today. 2007;12:1068–75.

34. Morishita M, Peppas NA. Is the oral route possible for peptide and protein drug delivery? Drug Discov Today. 2006;11:905–10.

35. Mohapatra S, Kar RK, Biswal PK, Bindhani S. Approaches of 3D printing in current drug delivery.

Sensors Int [Internet]. The Authors; 2022;3:100146. Available from: https://doi.org/10.1016/j.sintl.2021.100146

36. Lechanteur A, Plougonven E, Orozco L, Lumay G, Vandewalle N, Evrard B. Engineered-inhaled particles : Influence of carbohydrates excipients nature on powder properties and behavior. 2022;613.

37. Alhijjaj M, Belton P, Qi S. An investigation into the use of polymer blends to improve the printability of and regulate drug release from pharmaceutical solid dispersions prepared via fused deposition modeling (FDM) 3D printing. Eur J Pharm Biopharm. Elsevier B.V.; 2016;108:111–25.

38. Pires FQ, Alves-silva I, Pinho LAG, Chaker JA. Predictive models of FDM 3D printing using experimental design based on pharmaceutical requirements for tablet production. Int J Pharm [Internet]. Elsevier; 2020;588:119728. Available from: https://doi.org/10.1016/j.ijpharm.2020.119728

39. Infanger S, Haemmerli A, Iliev S, Baier A, Stoyanov E, Quodbach J. Powder bed 3D-printing of highly loaded drug delivery devices with hydroxypropyl cellulose as solid binder. Int J Pharm [Internet]. Elsevier; 2019;555:198–206. Available from: https://doi.org/10.1016/j.ijpharm.2018.11.048

40. Viidik L, Vesala J, Laitinen R, Korhonen O, Ketolainen J, Aruväli J, et al. Preparation and characterization of hot-melt extruded polycaprolactone-based filaments intended for 3D-printing of tablets. Eur J Pharm Sci. 2021;158.

41. Kim DH, Kim YW, Tin YY, Soe MTP, Ko BH, Park SJ, et al. Recent technologies for amorphization of poorly water-soluble drugs. Pharmaceutics. 2021;13.

42. Boniatti J, Januskaite P, da Fonseca LB, Viçosa AL, Amendoeira FC, Tuleu C, et al. Direct powder extrusion 3d printing of praziquantel to overcome neglected disease formulation challenges in paediatric populations. Pharmaceutics. 2021;13.

43. Izgelov D, Freidman M, Hoffman A. Investigation of cannabidiol gastro retentive tablets based on regional absorption of cannabinoids in rats. Eur J Pharm Biopharm [Internet]. Elsevier; 2020;152:229–35. Available from: https://doi.org/10.1016/j.ejpb.2020.05.010

44. Hughey JR, Keen JM, Miller DA, Kolter K, Langley N, McGinity JW. The use of inorganic salts to improve the dissolution characteristics of tablets containing Soluplus®-based solid dispersions. Eur J Pharm Sci [Internet]. 2013;48:758–66. Available from: http://dx.doi.org/10.1016/j.ejps.2013.01.004

45. Maggi L, Segale L, Torre ML, Ochoa Machiste E, Conte U. Dissolution behaviour of hydrophilic matrix tablets containing two different polyethylene oxides (PEOs) for the controlled release of a water-soluble drug. Dimensionality study. Biomaterials. 2002;23:1113–9.

46. Thiry J, Lebrun P, Vinassa C, Adam M, Netchacovitch L, Ziemons E, et al. Continuous

production of itraconazole-based solid dispersions by hot melt extrusion : Preformulation , optimization and design space determination. Int J Pharm [Internet]. Elsevier B.V.; 2016;515:114–24. Available from: http://dx.doi.org/10.1016/j.ijpharm.2016.10.003

47. Lin X, Su L, Li N, Hu Y, Tang G, Liu L, et al. Understanding the mechanism of dissolution enhancement for poorly water-soluble drugs by solid dispersions containing Eudragit® E PO. J Drug Deliv Sci Technol. 2018;48:328–37.

48. Hari SK, Gauba A, Shrivastava N, Tripathi RM, Jain SK, Pandey AK. Polymeric micelles and cancer therapy: an ingenious multimodal tumor-targeted drug delivery system. Drug Deliv Transl Res [Internet]. Springer US; 2023;13:135–63. Available from: https://doi.org/10.1007/s13346-022-01197-4

7. Abbreviation

API: active pharmaceutical ingredient

ASD: amorphous solid dispersion

CBD: cannabidol

DLS: dynamic light scattering

DPE: direct powder extrusion

E100: Eudragit® E100

FDM: fused-deposition modeling

HME: hot-melt extrusion

HPβCD: hydroxypropyl-β-cyclodextrin

PEG: polyethylene glycol

PEO: Polyox® WSR N10

SOL: Soluplus®

Appendix

Evaluation of degradation temperature of raw materials:

As shown of Figure 7, the mass loss of CBD starts at 220 °C while mass loss for EPO, PEO and SOL starts at 289 °C, 389 °C and 290 °C, respectively.

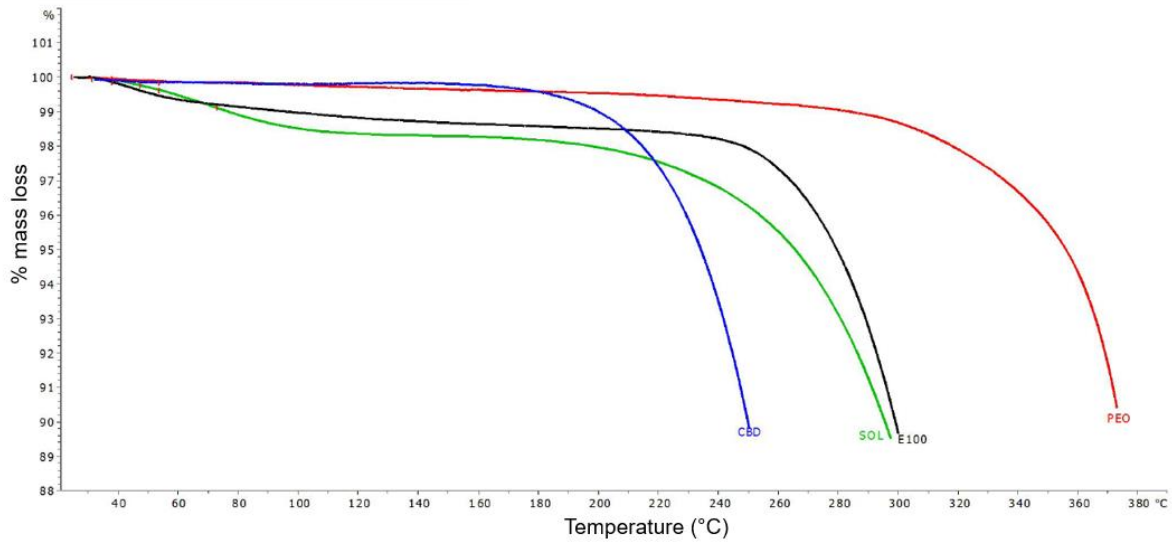

Figure 7 – Mass loss from 100% to 90% of the initial mass for CBD, E100, SOL and PEO after TGA analysis.